PHYSICAL REVIEW B **86**, 184423 (2012)

Spin-resolved characterization of single cobalt phthalocyanine molecules on a ferromagnetic support

J. Brede and R. Wiesendanger

Institute of Applied Physics and Interdisciplinary Nanoscience Center Hamburg, University of Hamburg, D-20355 Hamburg, Germany

(Received 21 July 2012; published 19 November 2012)

We report on spin-resolved measurements of single cobalt phthalocyanine molecules which are coupled to a ferromagnetic cobalt support. The same molecule is probed while the magnetization direction of the tip is rotated from parallel to antiparallel by the application of an external magnetic biasing field. Highly spin-polarized states near the Fermi energy demonstrate the realization of a single molecule spin filter. Intramolecular variations of the molecular spin polarization reveal a spin-polarized resonance for the molecular cobalt ion as well as a spin polarization carried by the organic ligand. The polarization measured for the molecular ion is of the same sign as the polarization of the cobalt support and has an opposite sign compared to the polarization measured for the molecular ligand. We argue that both effects arise due to a delicate balance in the hybridization between substrate states and molecular orbitals: surface and interface states, molecular ligand π orbitals, and molecular cobalt-ion d orbitals. Moreover, the degree of hybridization will influence the amount of charge transfer from the substrate into the unoccupied molecular orbitals, thereby affecting the molecular magnetic moment.

DOI: 10.1103/PhysRevB.86.184423 PACS number(s): 68.43.Fg, 73.20.At, 75.70.Rf, 85.65.+h

I. INTRODUCTION

Organic molecules are promising materials for transporting spin information because they are built up of light elements, and have a weak spin-orbit coupling and hyperfine interactions.[1] In molecular systems spin-relaxation times in excess of 10 μs were already observed in the 1970s[2] and long spin-diffusion lengths were observed in spin valve experiments.[3,4] The origin of the measured giant magnetoresistance in these latter experiments was discussed controversially.[5] In particular the role of the organic-ferromagnet interface motivated a lot of additional research.[6,7] These recent experiments revealed that newly formed molecule-ferromagnet hybrid states are present at the interface and that they determine the spin injection into the organic layer. Depending on the degree of hybridization of molecule and substrate, the newly formed hybrid states have an opposite sign of the spin polarization compared the underlying ferromagnet.[6–8] Moreover, organic molecules such as the macrocyclic phthalocyanine (PC) can be functionalized by various metal atoms to become magnetic. These magnetic molecules may be, if anchored to an appropriate surface, used to store, read, or manipulate magnetic information. Crucial toward the end of realizing such functional single molecule devices is the understanding of how different molecular constituents couple to their surrounding: especially the different coupling mechanisms of the molecular metal atoms and the organic ligand with the surface must be understood in order to design molecular devices down to the single molecule limit.

Ferromagnetic Co nanostructures were studied in numerous experiments and were proposed as promising templates for spintronic applications.[9] In particular, Co islands on Cu(111) have been studied intensively.[10,11] Co islands of various thickness were also deposited on Pt(111) surfaces and showed similar magnetic properties as Co islands on Cu(111). However, the significant lattice mismatch of Pt and Co induces the formation of dislocation lines on the Co islands on Pt(111) and gives rise to a highly nonuniform electronic structure.[12] Alternatively, Co islands of one atomic layer (AL) height can be grown on an Ir(111) substrate. These Co islands on Ir(111) exhibited predominantly one type of stacking and no dislocation patterns, indicating a pseudomorphic growth. They showed an easy axis of the magnetization normal to the surface and a remarkably high coercivity greater than 2 T.[9] These properties make the Co nanostructures on the Ir(111) surface an interesting prototypical hard magnet for spin valve experiments as the one performed here.

In 2008 Iacovita *et al.*[13] reported the application of spin-polarized (SP) scanning tunneling microscopy (STM) to visualize the spin polarization of single CoPC molecules in contact with ferromagnetic Co islands grown on a Cu(111) crystal. The CoPC molecules showed a spin-polarized electronic resonance below the Fermi energy. By comparison with first-principles calculations Iacovita *et al.* identified that the resonance arises due to a ferromagnetic coupling of the CoPC and the Co nanostructure. Two mechanisms were suggested to be responsible for the coupling: a direct exchange coupling of the Co ion inside the PC macrocycle to the Co atoms of the island underneath and a $\sim$90° superexchange mechanism of the Co ion via the inner molecular N atoms to the Co islands. Both favor a ferromagnetic coupling. It is interesting to note that the images presented in the work by Iacovita *et al.* suggest that the CoPC molecules studied were in close proximity to one another. Recent work by Tsukahara *et al.*[14] indicated that FePCs on a Au(111) surface couple magnetically via Ruderman-Kittel-Kasuya-Yosida (RKKY) interaction on a nonmagnetic Au(111) surface when they are about one nanometer apart. Moreover, Gopakumar *et al.*[15] showed that an ordered superstructure of FePCs on Ag(111) is partially electronically decoupled from the metal surface. While the relevant energy scale of the former work is much lower than the one for direct exchange interactions, the effect reported in the latter work is not to be disregarded, *a priori*. Furthermore, Iacovita *et al.* did not address the spin dependence of the same molecule, but relied on the comparison of structurally and electronically identical molecules situated on oppositely magnetized domains. Here, we demonstrate how magnetic contrast in the spin-resolved SP-STM images is unambiguously established by the application of an external magnetic

field and we proceed to record the spin dependence of a single CoPC molecule. Note that in the publication by Iacovita *et al.* the molecular spin polarization was experimentally observed close to the central Co ion. In contrast, more recent SP-STM experiments, in which the molecular spin polarization was resolved on a submolecular scale, clearly demonstrate that the organic molecular ligand can carry spin information as well.[16]

II. EXPERIMENTAL METHODS

Spin-sensitive tips were prepared by coating an *in vacuo* flash heated W tip with ∼50 monolayers (MLs) of Fe. Ir single crystals were cleaned *in vacuo* by argon ion etching (at an argon pressure of $p_{Ar} \approx 5 \times 10^{-6}$ mbar for a duration of $t = 30$ min), consecutive annealing at a temperature of $T = 700$–1200 K in an oxygen pressure (at $p_{O_2} \approx 1 \times 10^{-7}$ mbar for $t = 30$ min), and a final flash heating to a temperature $T \approx 1200$ K for a duration of $t = 210$ sec. Co was deposited *in vacuo* on the clean Ir(111) crystal at room temperature. Deposition was done via electron bombardment heating of a Co rod to evaporate material in a line of sight onto the sample surface. The sample was directly transferred *in situ* to the STM in order to minimize contamination of the Co islands. Then molecules were deposited from homebuilt Knudsen cells onto the precooled surface.[17] The deposition of molecules onto a cold surface hindered thermally induced mobility. The pressure during Co island and molecule deposition stayed always below $p < 2 \times 10^{-10}$ mbar. All measurements were performed with sample and tip at a temperature of ∼6.5 K.

All STM and SP-STM topographs were recorded in the constant current mode, i.e., the tip height is adjusted via a feedback loop to maintain a constant tunneling current value during scanning. The differential tunneling conductance dI/dU is recorded by superimposing a sinusoidal ac modulation voltage (frequency f_{mod}, amplitude U_{mod}) and recording the response of the tunneling current via lock-in technique. Point spectroscopy data were recorded by positioning the tip at predefined positions at fixed tip-sample distances (given by the stabilizing parameters I_{stab} and U_{stab}), disabling the feedback loop, sweeping the bias voltage in a preset range, while recording the dI/dU signal. All maps of the differential tunneling conductance (dI/dU maps) shown here were recorded simultaneously with STM topographs in the constant current mode.

III. EXPERIMENTAL RESULTS

A. Adsorption geometry

Figure 1 shows a topograph of a Co nanostructure and the Ir(111) surface: the sample is decorated with single, well separated CoPC molecules. Three distinct orientations are identified for CoPC molecules adsorbed on the Ir ($CoPC_{Ir}$) as well as for CoPC molecules situated on top of the Co nanostructure ($CoPC_{Co}$). While the $CoPC_{Ir}$ molecules show the typical cloverleaf shape (with C_{2v} symmetry), $CoPC_{Co}$ molecules show a clear reduction of symmetry to C_s. The symmetry of $CoPC_{Co}$ molecules can best be seen in the inset of Fig. 1(a): the vertical axis connecting the benzopyrolle groups [compare Fig. 1(b)] is a mirror axis of the molecule on the surface, while

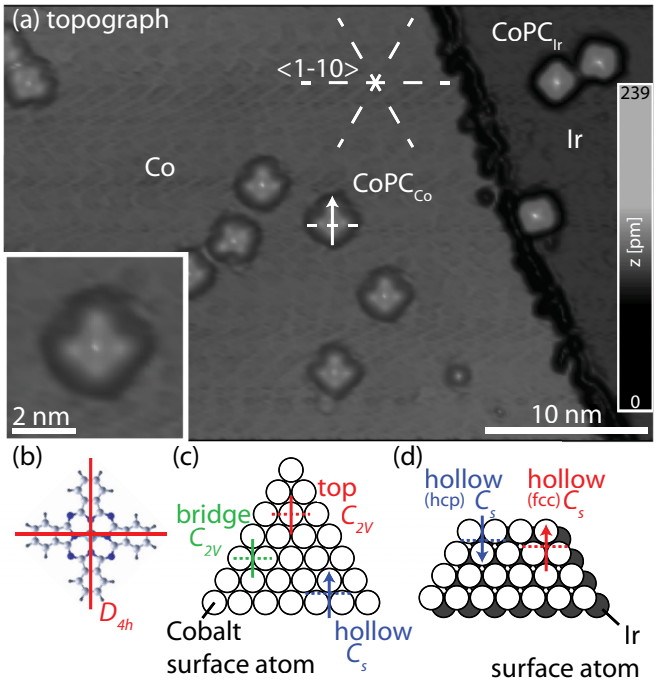

FIG. 1. (Color) CoPC molecules on Co nanostructures and on the Ir(111) surface. (a) High-resolution topograph of CoPC molecules on the Co nanostructure and on the Ir support. The molecules appear in a typical cross shape on both the Co and the Ir support. The CoPC molecules can be found in three distinct orientations, with two benzopyrrole groups oriented parallel to the close-packed rows of the atomic lattice underneath. The $CoPC_{Co}$ symmetry is reduced to C_s. The reduction from D_4 symmetry [as for the free molecule, compare (b)] to C_s can be understood when considering the top surface layer: only the hollow site reduces the symmetry of molecule + surface to C_s, while both top and bridge adsorption sites would preserve a C_{2v} symmetry. The observation of only three orientations can be understood if the second surface layer is considered, because it allows us to distinguish the hollow sites into hcp (with a second surface layer atom beneath) and fcc (no second surface layer atom beneath). Image parameters: $I = 0.2$ nA $U = 1000$ mV.

the horizontal axis is not. The reduction of molecular symmetry from D_4 (free CoPC) to C_s ($CoPC_{Co}$) can be understood if the top surface layer is considered: Fig. 1(c) shows the three different high-symmetry adsorption sites (i.e., the site where the Co ion of the $CoPC_{Co}$ is sitting); top and bridge sites retain a C_{2v}, while the hollow site reduces the symmetry to C_s. Note that a close-packed surface layer has two equivalent hollow sites, each exhibiting threefold symmetry, therefore one would expect six different adsorption geometries. The fact that only three of the six orientations are observed indicates that the second surface layer influences the adsorption: either the fcc or the hcp site is energetically more favorable.

B. Spin-sensitive studies

After the adsorption geometry of $CoPC_{Co}$ molecules has been established we study the spin-dependent properties of the system. In a first step magnetic contrast is established by the application of an external magnetic field B_{ext}, using the Co nanostructures as a reference: the nanostructures exhibit a strong magnetic contrast in the spin-resolved dI/dU maps at

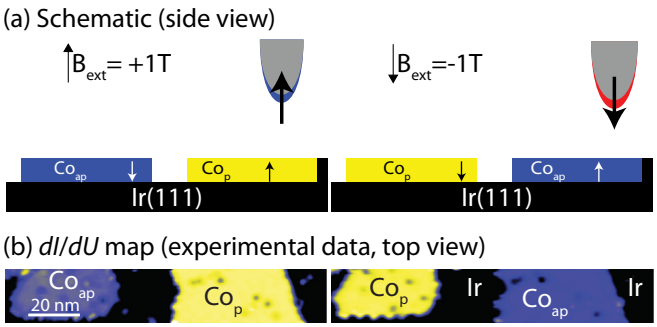

FIG. 2. (Color) Schematic of spin-resolved measurements of CoPC molecules on Co on Ir(111). An external magnetic biasing field is applied along the z axis: the tip magnetization direction is either parallel (p) or antiparallel (ap) to the Co nanostructures. (a) Schematic illustration of the measurement; (b) shows experimental dI/dU data. Left column: when $B_{\text{ext}} = 1$ T is applied the tip magnetization is ap to the left Co structure, resulting in a low (blue) spin-resolved tunneling conductance, while it is p with respect to the right Co structure, leading to a high (yellow) spin-resolved tunneling conductance. The situation is reversed as the polarity of the external magnetic biasing field is reversed (right column). Thus magnetic contrast is unambiguously established. Imaging parameters: $I = 2$ nA, $U = -500$ mV, $U_{\text{mod}} = 20$ mV$_{\text{rms}}$, $f_{\text{mod}} = 3.3333$ kHz.

a bias voltage of $U = -500$ mV. Two Co nanostructures with opposite magnetic contrast (dark blue and yellow) are visible in Figs. 2(a) and 2(b). This contrast is due to their opposite magnetization directions. The Co nanostructures reverse their magnetic contrast as the tip magnetization is reversed in an external magnetic field (going from $B = -0.6$ T [Fig. 1(a)] to $B = +0.6$ T [Fig. 1(b)], while the nonmagnetic Ir(111) surface (black) does not change its contrast. This behavior unambiguously demonstrates the spin dependence of the tunneling current and thereby establishes magnetic sensitivity of the tip.

C. Spin- and energy-dependent characterization of single CoPC molecules from topographs

After spin sensitivity of the tip was ascertained we proceeded to map the spin dependence of single CoPC molecules in two complementary approaches. Figure 3 shows spin-resolved topographs. Before addressing the spin information in these images, we will focus on the bias dependent appearance of the molecules. The change of molecular appearance with bias voltage applied gives a hint as to which molecular orbitals are involved in the tunneling processes at the given bias voltage. It is instructive to compare the CoPC molecules on Co with the ones adsorbed on Ir. At a positive bias voltage (which means probing the unoccupied molecular states) of $U = 1000$ mV applied [Fig. 3(a)] CoPC$_{\text{Co}}$ as well as CoPC$_{\text{Ir}}$ show a significant contribution from the molecular center (i.e., the Co ion) which gives rise to the central maximum in the STM topographs. The contribution from the molecular ligand leads to the four cloverleafs around the central maximum. When imaged at a bias voltage of $U = -100$ mV (which corresponds to probing the occupied molecular states) CoPC$_{\text{Co}}$ appears with a pronounced central maximum (which is accompanied with an increase in apparent height of ∼50–70 pm [see line

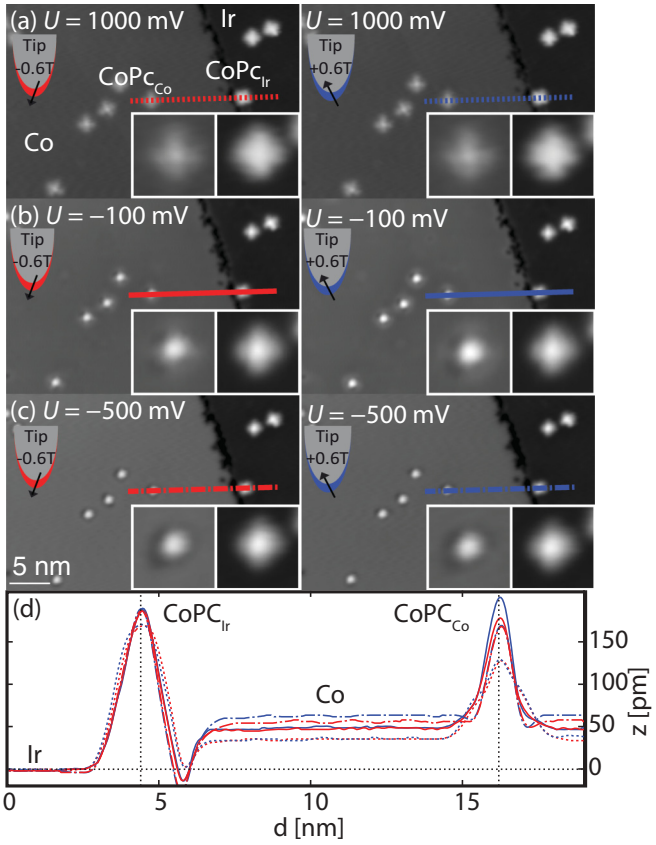

FIG. 3. (Color) Spin-dependent topographs and line profiles of CoPC molecules on Co nanostructures and the Ir(111) surface. (a)–(c) Left panels show the same local sample area imaged at different bias voltages (as indicated) with an external magnetic field of −0.6 T applied [insets shows a zoom of a CoPC molecule on Co (left) and on Ir(111) (right)]. (a)–(c) Right panels show the same area as shown in the left panels, but with an external magnetic field of +0.6 T applied. (d) Line profiles as indicated in (a)–(c), i.e., the same line profile, across the Ir surface, a CoPC$_{\text{Ir}}$ molecule, the Co nanostructure, and a CoPC$_{\text{Co}}$ molecule, is measured for different bias voltages applied (dotted line at $U = 1000$ mV, solid line at $U = -100$ mV, and the dashed-dotted line at $U = -500$ mV and different external magnetic fields; red (blue) lines give data for $B_{\text{ext}} = -0.6$ T ($B_{\text{ext}} = +0.6$ T). All images: $I = 0.2$ nA.

profiles as given in Fig. 3(d)], while there is almost no signal from the molecular ligand. Contrarily, CoPC$_{\text{Ir}}$ still exhibits the four outer features from the molecular ligand (as well as the central maximum). The differences in appearance of the molecular ligand indicate that the molecular orbitals—giving rise to the cloverleaf shape—of CoPC$_{\text{Co}}$ are energetically shifted compared to CoPC$_{\text{Ir}}$. This can be intuitively understood considering the difference in work function of ∼300 meV between Co and Ir,[18] which leads to a shift of the onset of molecular orbitals depending on the substrate. Most likely there are other factors which will significantly influence the energetic position of molecular orbitals: it is to be expected that the interaction between the CoPC$_{\text{Co}}$ molecules and the Co nanostructure is significantly stronger than for CoPC$_{\text{Ir}}$ and the less reactive Ir surface. Strong hybridization of molecular orbitals and surface states leads to a significant broadening of MOs, to charge transfer, and a possible pinning of the highest

occupied molecular orbital (HOMO) to the Fermi energy.[19] Generally, complex rearrangements of the molecular orbitals are expected for the molecule-metal hybrid states. Indeed, these processes were recently discussed theoretically in detail for CoPC molecules on Co compared to CoPC molecules on Cu.[19] Note that $CoPC_{Ir}$ molecules generally appear higher [by about 50 pm; see also the line profiles as given in Fig. 3(d)] compared to $CoPC_{Co}$, this concurs with the interpretation that the interaction between the molecule and the Ir surface is weaker than the interaction between molecule and the Co nanostructure. Moreover, the sharp increase in apparent height for $CoPC_{Co}$ at the molecular center (when imaged at negative bias voltages) shows that a molecular orbital at the molecular Co-ion site is available for tunneling and that this state extends far into the vacuum. Therefore, the HOMO of $CoPC_{Co}$ is identified as a $d_{3z^2-r^2}$-type orbital.

Next, the spin-dependent changes in apparent height are discussed: at a bias voltage of $U = 1000$ mV applied, the $CoPC_{Co}$ molecules have a maximum apparent height [relative to the Ir surface, measured at the molecular center; see Fig. 3(d)] of ∼120 pm and $CoPC_{Ir}$ molecules of ∼160 pm. The apparent height for both $CoPC_{Co}$ and $CoPC_{Ir}$ molecules is the same for both magnetic-field directions applied. The situation is very different at a bias voltage of $U = -100$ mV applied. While $CoPC_{Ir}$ molecules show only a slight increase in apparent height to ∼170 pm, independent of external magnetic field applied, $CoPC_{Co}$ molecules show a significant increase in apparent height for $B_{ext} = +0.6$ T to ∼190 pm and to ∼170 pm when $B_{ext} = -0.6$ T. This field dependence of the apparent height shows that the previously identified $d_{3z^2-r^2}$-type orbital is strongly spin polarized. It was shown that the difference in apparent height (∼20 pm) depending on the relative orientation of tip and sample is a measure for the integrated local effective spin polarization.[16,20] For an applied bias voltage of $U = -500$ mV the Co nanostructure shows a profound dependence on the relative tip and sample magnetization directions, which is reflected in the apparent height difference of ∼10 pm, while $CoPC_{Co}$ and $CoPC_{Ir}$ molecules show no spin dependence at this energy.

D. Maps of the local spin polarization

In order to map the spatial distribution of the spin polarization we calculate maps of the integrated local effective spin polarization (SP map) following the method described before.[16,20] For comparison we have simultaneously deduced maps of the dI/dU asymmetry (dI/dU_{asym}-maps).[21] The maps of the integrated local effective spin polarization provide insight into the energy integrated spin polarization of the sample measured at the position of the tip, where the interval of integration is defined by $[E_F, E_F + eU]$. On the one hand, the dI/dU asymmetry gives energy selective [at an energy given by the bias voltage applied (eU)] insight into the local effective spin polarization, on the other hand, it suffers from topographic effects.[22] These topographic effects make a correlation between the dI/dU asymmetry and the local effective spin polarization difficult. In general it requires additional tedious measurements to associate the dI/dU asymmetry and the local effective spin polarization.

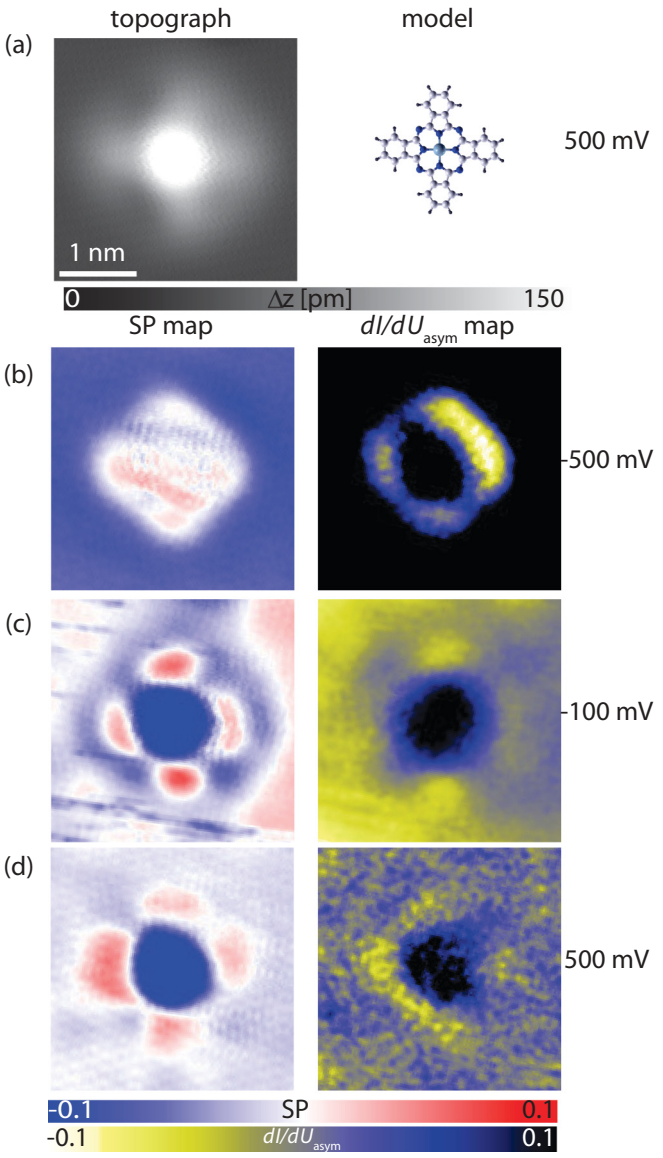

FIG. 4. (Color) Maps of the integrated local effective spin polarization and of the dI/dU asymmetry. (a) Topograph and model geometry of a CoPC molecule on a Co nanostructure. (b) At a bias voltage of $U = -500$ mV no spin polarization is observed for $CoPC_{Co}$, while the Co nanostructure shows a strong negative polarization. (c) At a bias voltage of $U = -100$ mV a strong negative spin polarization is visible for the Co ion and a positive spin polarization for the carbon rings of $CoPC_{Co}$. A halo of negative polarization is clearly visible around the $CoPC_{Co}$. The Co nanostructure shows almost no polarization. (d) with a bias voltage of $U = -500$ mV applied, there is still a strong negative polarization present at the Co ion and a weak positive spin polarization at the carbon rings of $CoPC_{Co}$. The Co nanostructure shows almost no polarization. All images were taken at $I = 0.2$ nA.

When a bias voltage of $U = -500$ mV is applied, the map of the integrated local effective spin polarization [Fig. 4(b), left panel] shows only the negative spin polarization of the Co substrate (SP ≈ −0.1), while the molecule does not show any signal (SP ≈ 0). Note that this implies that the tip-sample distance above the molecule is the same, independent of the polarity of the external magnetic field applied here,

thereby rendering it a good stabilization voltage for SP-STS measurements.[22] The dI/dU asymmetry map at this energy [Fig. 4(b), right panel], shows a strong positive signal from the Co nanostructure, a strong positive signal from the central part of the $CoPC_{Co}$ molecule, and a complex pattern on the molecular ligand: a negative signal at the upper two carbon units, while the other two show no prominent signal.

At a bias voltage of $U = -100$ mV applied, the SP map [Fig. 4(c) left panel] of $CoPC_{Co}$ molecules shows almost no spin polarization on the cobalt nanostructure (SP ≈ 0), a strong negative signal at the central part of the $CoPC_{Co}$ molecule (SP ≈ -0.2), a positive signal for the molecular ligand (SP ≈ -0.05) (primarily above the carbon rings), and another negative signal around the molecule (SP ≈ -0.1). The dI/dU asymmetry map shows a negative signal for the cobalt nanostructure, a positive signal at the central part of the $CoPC_{Co}$ molecule, and a weak negative signal on the organic ligand.

At a bias voltage of $U = 500$ mV applied, the SP map [Fig. 4(b), left panel] of $CoPC_{Co}$ molecules shows almost no spin polarization on the cobalt nanostructure (SP ≈ 0), a strong negative signal at the central part of the $CoPC_{Co}$ molecule (SP ≈ -0.1), a positive signal (SP ≈ 0.05) for the molecular ligand (primarily above the carbon rings). The dI/dU asymmetry map shows no significant signal for the cobalt nanostructure and a positive signal at the central part of the $CoPC_{Co}$ molecule.

The main observations that can be deduced from the SP maps are that the integrated local effective spin polarization for the central part of the molecule is of spin-down type while it is of spin-up type for the organic ligand, and a circular negative polarization is detected around the molecule at a bias voltage of $U = -100$ mV applied.

E. Spin-polarized point spectroscopy

In a second step, spin-resolved point spectroscopy data are recorded on the same $CoPC_{Co}$ molecule that is addressed above. The spectra are taken at the center of the molecule (i.e., above the Co atom) and on defect-free surface areas (i.e., with a distance greater than 2 nm to the next molecule, step edge, or point defect). Moreover, the stabilization parameters were chosen to have the same tip-sample distance for both parallel and antiparallel magnetization direction alignments: this method elegantly removes topographic effects in the dI/dU asymmetry.[22] Figure 5 shows data with different external magnetic fields applied. The red/blue lines give the data for parallel (p)/antiparallel (ap) tip and sample magnetization alignment. Figure 5(a) shows that $CoPC_{Co}$ molecules have a broad spin-polarized resonance just below the Fermi energy. For an antiparallel alignment of tip and sample magnetization directions (blue curve) two peaks can be identified: one at $U \approx -170$ mV and the other at $U \approx 0$ mV. Spectra of the Co nanostructure [Fig. 5(b)] show a characteristic spin-polarized peak in the differential tunneling conductance at $U \approx -260$ mV in agreement with previous work.[9] Similar spectroscopic features were reported for Co nanostructures, islands, and films on Cu, Pt, and W substrates.[10,23,24] This feature is generally attributed to a d-type surface state of spin-down character. The spin polarization [plotted in Fig. 5(c)] changes its sign from negative to positive at ≈ -350 mV (≈ -250 mV) for the Co nanostructure ($CoPC_{Co}$ molecule).

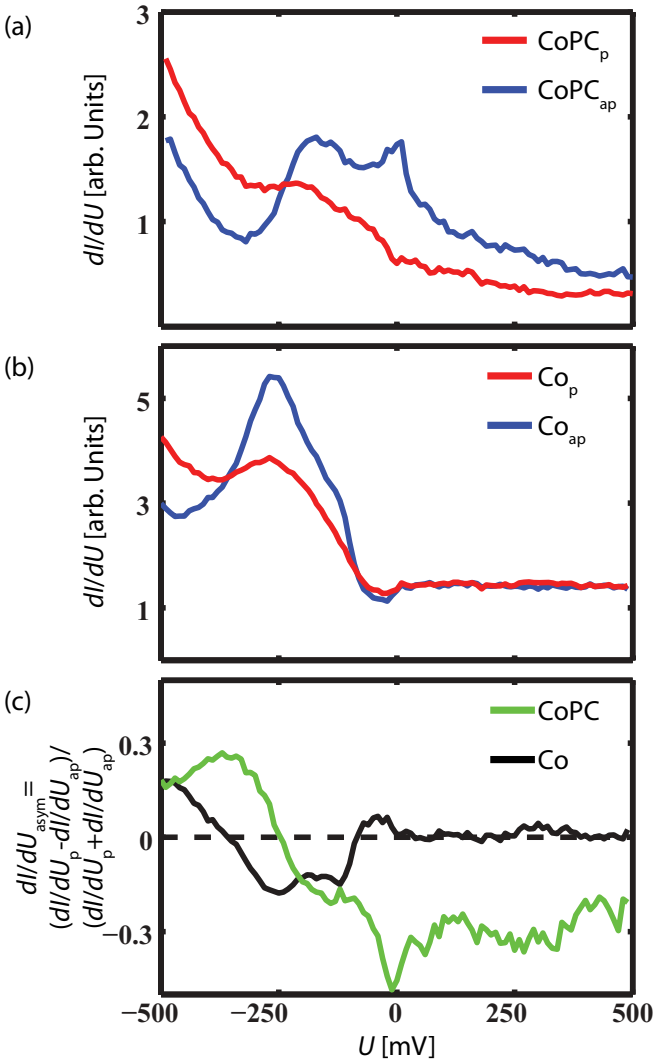

FIG. 5. (Color) Spin-resolved tunneling spectra. Every line represents the average over 12 individual spectra; the stabilization parameters are $I_{stab} = 0.2$ nA $U_{stab} = -500$ mV for (a) and $I_{stab} = 0.2$ nA $U_{stab} = 500$ mV for (b) and $U_{mod} = 15$ mV_{pp} $U_f = 1.111$ kHz. (a) Spin-resolved tunneling spectra of the $CoPC_{Co}$ show a broad spin-polarized resonance below the Fermi energy. For $CoPC_{ap}$ two peaks are visible: one centered at ~ -170 mV and one at the Fermi energy (0 mV). (b) the Cobalt nanostructure shows a characteristic spin-polarized peak at $U \approx -260$ mV. (c) The asymmetry shows how the spin polarization changes its sign from spin-down to spin-up at ~ -350 mV (~ -250 mV) for the Co nanostructure and the $CoPC_{Co}$ molecule, respectively.

IV. COMPARISON WITH CoPC ON Co/Cu(111) AND CoPC ON Fe/W(110)

First, we compare the results discussed above with the work by Iacovita *et al.*[13] for CoPC molecules on two atomic layer high cobalt islands on Cu(111). The atomic lattices of Cu and Ir are similar; they differ only by a difference in lattice spacing of $\sim 6\%$. Since the growth of the cobalt structures is pseudomorphic with the support in both studies, we assume

that we have similar cobalt lattices, i.e., they differ only in the lattice spacing by about 6%, whereas the symmetry is identical in both cases. There was no experimental determination of the adsorption site for $CoPC_{Co}$ in the publication by Iacovita *et al.*, theoretically the bridge site was determined to be the most favorable. In other studies the adsorption site for CoPC on Cu(111) was shown to be the bridge site.[25,26] Note that for CoPC on Cu(111) a symmetry reduction to C_{2v} (and not C_s, as is the case in this work) was observed. Thereby, the symmetry argument to determine the adsorption position, which was presented above in Sec. III A is in complete agreement with experimental observations. This leads to an interesting difference for the $CoPC_{Co}$ adsorption site on the two different cobalt lattices: a bridge site (deduced from first-principles calculations) was reported in the work of Iacovita *et al.*, while we determine (deduced from symmetry considerations) a hollow site. This implies that the slight stretching of the cobalt layer or the second surface layer significantly influences the molecular adsorption site. We favor (for the reasons outlined in Sec. III A) that it is the second surface layer which is the driving factor. Additional first-principles calculations for CoPC on 1 AL of Co on Ir(111) or a study of CoPC on 2 AL of Co on Ir(111) should answer the open questions about the adsorption site. Next, let us compare the spin-polarized resonance observed both by Iacovita *et al.* as well as in this work: In both cases a similar resonance is observed in the SP-STS data. Interestingly, the resonance seems to be shifted more toward the Fermi energy (by ∼60 meV) for CoPC on Co on Ir than for CoPC on Co on Cu. This shift in the onset of the CoPC resonance is of the same order as the shift for the surface state observed on the Co islands [∼−310 meV for Co on Cu (Ref. 10) and ∼−250 meV for Co on Ir (Ref. 9)]. This shift in onset energy for the states correlates with the difference in work functions for Cu and Ir.[18] We speculate that this shift in energy of the molecular cobalt resonance leads to a change in the molecular magnetic moment as well. The question about the magnetic moment needs to be addressed theoretically, because the measurements of the type presented here (or by Iacovita *et al.*) do not have access to the total magnetic moment. The second feature observed in this work, the spin polarization on the organic molecular ligand, which is of opposite sign as the spin polarization of the molecular cobalt ion, was not seen experimentally by Iacovita *et al.* in their publication, but it was proposed from first-principles calculations. Iacovita *et al.* argue that the magnetization induced in the organic ligand is too weak and below their experimental detection limit. The fact that it is clearly visible in our experiments indicates that the effect on the ligand is stronger when CoPC molecules are on Co on Ir. We propose that the observation of the spin polarization for the organic ligand is due to a stronger adsorption and increased interaction of molecule and substrate. Whether this increased interaction is due to a reduced molecule-surface distance, an influence of the Ir substrate, or possibly a subtle result of the increased lattice spacing will need additional experimental and theoretical investigations.

Second, we compare the results of this work with the publication for CoPC molecules on Fe on W(110).[16] CoPC molecules on Fe on W(110) are adsorbed in a top site and the W(110) lattice has a drastically different symmetry and packing than the close-packed Ir(111) surface. Therefore a direct comparison of the adsorption site gives little additional information. Please note that the molecular adsorption is not dominated by the adsorption site of the molecular cobalt ion, but rather by the minimization of the energy of all atoms constituting the phthalocyanine, i.e., the adsorption position of the various carbon and nitrogen atoms was shown to be the driving force when determining the adsorption site of the simple organic molecules.[8] These molecules align in such a way that the maximum number of carbon atoms and carbon (double) bonds sit directly above Fe surface atoms.[8] Not only is the adsorption site of the molecular Co ion drastically different, but also the electronic structure of the Fe film differs significantly from the properties of the Co nanostructures. Nevertheless, first-principles calculations determined two $d_{3z^2-r^2}$-type surface states for a 2-AL-thick Fe film: one is situated at ∼−180 meV below the Fermi edge.[27] This state was observed in SP-STM experiments as well,[27] indicating a slow decay of this state into the vacuum and it is therefore at similar energies and exhibits similar properties as the $d_{3z^2-r^2}$ state present in the Co nanostructures. Therefore, it is striking that the measured spin polarization for the Co ion on a CoPC on 2 AL of Fe on W(110) is drastically different from the one reported here, e.g., there is no polarization close to the Fermi edge and a change in sign in the polarization is present when tunneling into unoccupied compared to tunneling out of occupied sample states. A possible explanation for this behavior is given by the first-principles calculations for CoPC on Fe on W(110):[16] the calculations determined a complete charge transfer between molecule and surface, which leads to a quenching of the molecular moment upon adsorption. The different amount of charge that is transferred for the different substrates leads to a rearrangement of molecular orbitals, which can explain the experimental observation. Interestingly, CoPC on Fe on W(110) shows a very strong polarization on the molecular ligand; the effect is even stronger than for CoPC on Co on Ir(111) and is observable in a wider energy range. We speculate that we have a stronger interaction of molecule and substrate on the Fe film compared to the Co film, which leads to an enhancement of the spin polarization for the ligand.

The comparison of CoPC on these three different surfaces indicate that the $d_{3z^2-r^2}$ state of the cobalt nanostructures plays a crucial role for determining the energetic position of the of the molecular Co ion $d_{3z^2-r^2}$ resonance. The energetic position of the molecular resonance, in turn, indicates that a different amount of charge is being transferred. Moreover, with increasing adsorption energy of the molecules, the effect of the induced molecular spin polarization on the organic ligand is enhanced.

V. CONCLUSIONS

In summary, the adsorption configuration and the magnetic interaction of single CoPc molecules on ferromagnetic Co nanostructures of one atomic layer thickness on an Ir(111) surface are addressed. CoPC molecules on top of the Co nanostructures appear with a reduced (C_s) symmetry. The reduced symmetry indicates an adsorption with the molecular Co ion situated in a hollow site of the Co lattice underneath. The observation of only three symmetry related orientations suggests that the second surface layer influences the adsorption, i.e.,

either a fcc or a hcp site is preferred. A controlled rotation of the magnetization direction of the SP-STM tip with an external magnetic field enables the study of the spin-dependent properties of the same $CoPC_{Co}$ molecule. Therefore, the data evaluation does not rely on the intercomparison of similar molecules on oppositely magnetized domains. Moreover, the data obtained for $CoPC_{Ir}$ molecules does not reveal any spin dependence; this is either because the magnetization direction of the molecule is not fixed, or because the magnetic moment of the molecule is quenched upon adsorption. Spin-resolved measurements show for $CoPC_{Co}$ molecules a highly spin-polarized state at a bias voltage of $U = -100$ mV applied. This state is spatially primarily localized at the molecular Co-ion site. The spatial confinement and the significant decay into the vacuum suggest that the spin-polarized feature primarily stems from a molecular $d_{3z^2-r^2}$-state contribution. Moreover, a weak integrated local effective spin polarization of opposite sign is observed for the organic ligand of the molecule. This was predicted for CoPC on 2 ML Co on Cu(111) theoretically, but was not observed experimentally, before. Last, a circular spin-polarized feature is observed around the $CoPC_{Co}$ molecules at $U \approx -100$ mV. The origin of this feature is not yet clear. It could arise due to the screening of the charged $CoPC_{Co}$ molecule by the spin-polarized conduction electrons in the Co nanostructure. While the origin of this feature needs to be confirmed by additional experimental and theoretical work, the mere presence of the feature demonstrates clearly that the presence of the molecule directly influences the electronic and magnetic properties of the Co layer in the immediate vicinity, highlighting the importance of studying well isolated molecules. The $CoPC_{Co}$ molecule acts as a technologically interesting efficient spin filter, because the local effective spin polarization is enhanced close to the Fermi energy when compared to the Co islands. This highlights the possibility to engineer the spin properties of molecule-ferromagnet interfaces through the adsorption of molecular systems. A systematic comparison with other spin-resolved studies for CoPC molecules shows that the surface and interface states can be used to pin the $d_{3z^2-r^2}$-type resonances of the Co ion of the molecule relatively to the Fermi energy. Furthermore, we see compelling evidence that an increase of the adsorption strength leads to an enhancement of the spin polarization on the organic ligand of the CoPC. Our findings demonstrate that molecule-ferromagnet hybrid systems can be engineered by tuning the surface reactivity and exploiting surface as well as interface resonances of appropriate symmetry. Thereby, additional ways to tune the spin filter effects present in magnetic and organic molecules become accessible.

ACKNOWLEDGMENTS

Financial support from the Deutsche Forschungsgemeinschaft via SFB 668, from the EU via the ERC Advanced Grant FURORE, and from the Cluster of Excellence NANOSPINTRONICS, funded by the Forschungs- und Wissenschaftsstiftung Hamburg, is gratefully acknowledged.

[1] A. R. Rocha, V. M. Garcia-suarez, S. W. Bailey, C. J. Lambert, J. Ferrer, and S. Sanvito, Nat. Mater. **4**, 335 (2005).

[2] C. B. Harris, R. L. Schlupp, and H. Schuch, Phys. Rev. Lett. **30**, 1019 (1973).

[3] V. Dediu, M. Murgia, F. C. Matacotta, C. Taliani, and S. Barbanera, Solid State Commun. **122**, 181 (2002).

[4] Z. H. Xiong, D. Wu, Z. Valy Vardeny, and J. Shi, Nature (London) **427**, 821 (2004).

[5] J. S. Jiang, J. E. Pearson, and S. D. Bader, Phys. Rev. B **77**, 035303 (2008).

[6] C. Barraud, P. Seneor, R. Mattana, S. Fusil, K. Bouzehouane, C. Deranlot, P. Graziosi, L. Hueso, I. Bergenti, V. Dediu *et al.*, Nat. Phys. **6**, 615 (2010).

[7] N. Atodiresei, J. Brede, P. Lazić, V. Caciuc, G. Hoffmann, R. Wiesendanger, and S. Blügel, Phys. Rev. Lett. **105**, 066601 (2010).

[8] N. Atodiresei, V. Caciuc, P. Lazić, and S. Blügel, Phys. Rev. B **84**, 172402 (2011).

[9] J. E. Bickel, F. Meier, J. Brede, A. Kubetzka, K. von Bergmann, and R. Wiesendanger, Phys. Rev. B **84**, 054454 (2011).

[10] O. Pietzsch, A. Kubetzka, M. Bode, and R. Wiesendanger, Phys. Rev. Lett. **92**, 057202 (2004).

[11] O. Pietzsch, S. Okatov, A. Kubetzka, M. Bode, S. Heinze, A. Lichtenstein, and R. Wiesendanger, Phys. Rev. Lett. **96**, 237203 (2006).

[12] F. Meier, K. von Bergmann, J. Wiebe, M. Bode, and R. Wiesendanger, J. Phys. D: Appl. Phys. **40**, 1306 (2007).

[13] C. Iacovita, M. V. Rastei, B. W. Heinrich, T. Brumme, J. Kortus, L. Limot, and J. P. Bucher, Phys. Rev. Lett. **101**, 116602 (2008).

[14] N. Tsukahara, S. Shiraki, S. Itou, N. Ohta, N. Takagi, and M. Kawai, Phys. Rev. Lett. **106**, 187201 (2011).

[15] T. G. Gopakumar, T. Brumme, J. Kröger, C. Toher, G. Cuniberti, and R. Berndt, J. Phys. Chem. C **115**, 12173 (2011).

[16] J. Brede, N. Atodiresei, S. Kuck, P. Lazić, V. Caciuc, Y. Morikawa, G. Hoffmann, S. Blügel, and R. Wiesendanger, Phys. Rev. Lett. **105**, 047204 (2010).

[17] In later experiments molecules were deposited on the sample held at room temperature. Still, even under these preparation conditions single well isolate molecules are found on the surface.

[18] H. B. Michaelson, J. Appl. Phys. **48**, 4729 (1977).

[19] X. Chen and M. Alouani, Phys. Rev. B **82**, 094443 (2010).

[20] R. Wiesendanger, H.-J. Güntherodt, G. Güntherodt, R. J. Gambino, and R. Ruf, Phys. Rev. Lett. **65**, 247 (1990).

[21] The dI/dU asymmetry is defined as

$$dI/dU_{\text{asym}}(eU) = \frac{dI/dU_p(eU) - dI/dU_{ap}(eU)}{dI/dU_p(eU) + dI/dU_{ap}(eU)}.$$

[22] A. Kubetzka, O. Pietzsch, M. Bode, and R. Wiesendanger, Appl. Phys. A **76**, 873 (2003).

[23] F. Meier, K. von Bergmann, P. Ferriani, J. Wiebe, M. Bode, K. Hashimoto, S. Heinze, and R. Wiesendanger, Phys. Rev. B **74**, 195411 (2006).

[24] J. Wiebe, L. Sacharow, A. Wachowiak, G. Bihlmayer, S. Heinze, S. Blügel, M. Morgenstern, and R. Wiesendanger, Phys. Rev. B **70**, 035404 (2004).

[25] S.-H. Chang, S. Kuck, J. Brede, L. Lichtenstein, G. Hoffmann, and R. Wiesendanger, Phys. Rev. B **78**, 233409 (2008).

[26] B. W. Heinrich, C. Iacovita, T. Brumme, D.-J. Choi, L. Limot, M. V. Rastei, W. A. Hofer, J. Kortus, and J.-P. Bucher, J. Phys. Chem. Lett. **1** 1517 (2010).

[27] M. Bode, S. Heinze, A. Kubetzka, O. Pietzsch, X. Nie, G. Bihlmayer, S. Blügel, and R. Wiesendanger, Phys. Rev. Lett. **89**, 237205 (2002).